to the change in frequency. Therefore, calculations of the frequency changes of the distorted ring conformations have been performed by varying the rotation of the $-CH_2CH_2CH_2-$ part (or equivalently of the Co atom) in an interval between 0 to 12° in the skew-boat form and −6 to +6° in the chair form. The coordinates of the hydrogen atoms attached to the nitrogen were obtained by rotation around the Co–N axis by appropriate angles. Results of such calculations are summarized in Table I. It can be seen that some normal modes are found to be rather sensitive to the conformational distortion. However, no considerable frequency change was found upon such distortion for the normal modes of interest.

The conformational analysis indicates further that the chair conformation should be preferred energetically over the skew-boat one. This is due to larger torsional strains around the N–C and C–C bonds in the latter. Moreover, nonbonded interactions between the chelates and the apical ligands in the *trans*-bis(1,3-propanediamine) complexes contribute, even though only in small measure, to the energy difference between chair and skew-boat rings. Hence, the conformers presented in Figure 4 rise energetically in the order i < ii < iii < iv < v, according to the total number of skew-boat rings involved in the complexes. Assuming a Boltzmann distribution, the molar fractions of trans complexes in these particular conformations fall monotonically in the same order. Thus, if in the solution only some fraction of trans complexes containing a skew-boat ring or rings would be present, form iii should be found to be more stable than configurations iv and v, which are much higher in energy. This is apparently not the case; instead, in the case of tris(1,3-propanediamine) complexes the infrared-active vibration at 950 cm^{-1} in the spectra of $[Co(tn)_3]^+$ and $[Cr(tn)_3]^+$ is seen. Since this frequency has been previously attributed to a skew-boat form of the six-membered ring, some fraction of $[M(tn)_3]^{3+}$ (M = Cr, Co) in D_2O seems to have a structure in which the six-membered ring or rings adopt a skew-boat conformation.

Registry No. *trans*-$[Co(NO_3)_2(tn)_2]NO_3$, 22545-85-3; *trans*-$[CoCl_2(tn)_2]Cl$, 31107-58-1; *trans*-$[Co(CN)_2(tn)_2]Cl{\cdot}H_2O$, 103531-52-8; *trans*-$[Co(CN)_2(tn)_2]Cl{\cdot}3H_2O$, 103531-53-9; $[Cr(tn)_3][Ni(CN)_5]{\cdot}2H_2O$, 52154-76-4; $[Cr(tn)_3]Cl_3$, 17978-78-8; $[Co(tn)_3]Cl_3$, 15242-48-5; D_2, 7782-39-0; tn, 109-76-2; Co, 7440-48-4.

(24) Matsumoto, K.; Kawaguchi, H.; Kuroya, H.; Kawaguchi, S. *Bull. Chem. Soc. Jpn.* **1973**, *46*, 2424.
(25) Herak, R.; Celap, M. B.; Krstanovic, I. *Acta Crystallogr., Struct. Crystallogr. Cryst. Chem.* **1975**, *B33*, 3368.
(26) Srdanov, G.; Herak, R.; Prelesnik, B. *Inorg. Chim. Acta* **1979**, *33*, 23.

Contribution from the Department of Chemistry, Washington University, St. Louis, Missouri 63130

An Open-Mode Nickel Dimer Based on a Binucleating Hexaphosphine Ligand System. Solid-State and Solution Conformations

Scott A. Laneman and George G. Stanley*[1]

Received August 22, 1986

Our interest in exploring the possibilities for dimer systems as homogeneous catalysts have led to the design and synthesis of a hexakis(tertiary phosphine) ligand, $(Et_2PCH_2CH_2)_2PCH_2P(CH_2CH_2PEt_2)_2$ (eHTP), which has the ability to both bridge and bis chelate two transition-metal centers in either a closed-mode M–M bonded form (**1a**) or in one of several open-mode conformations (**1b** or **1c**) (assuming that bis chelation will be a driving coordination factor). We have recently reported the synthesis and characterization of the open-mode cobalt dimer $Co_2(CO)_4(eHTP)^{2+}$ (**2**), which has the unique inverted W-shaped eHTP coordination geometry **1b**.[2] We would now like to report two additional variations on the open-mode conformations of eHTP involving nickel(II) eHTP complexes.

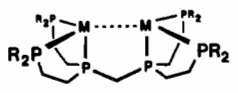

1a

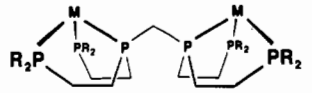

1b

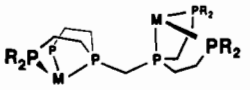

1c

Experimental Section

Unless otherwise stated all procedures were carried out under inert atmosphere (prepurified nitrogen or argon) using standard Schlenk line or glovebox techniques. eHTP was prepared according to published procedures.[2] IR spectra were run on a Perkin-Elmer 283B spectrometer. The 300-MHz NMR spectra were performed on a Varian CXP-300 FT spectrometer and referenced to solvent peaks.

Preparation of $Ni_2Cl_2(eHTP)^{2+}(X^-)_2$ (3). A 1.018-g (1.87-mmol) sample of eHTP in 20 mL of degassed EtOH was added dropwise to 0.888 g (3.74 mmol) of $NiCl_2{\cdot}6H_2O$ in 20 mL of degassed EtOH under inert atmosphere conditions. The solution rapidly turned from green to dark brown-red. After the addition was complete the solution was stirred for 5 min and vacuum evaporated to dryness to form crude $Ni_2Cl_2(eHTP)^{2+}(Cl^-)_2$ (**3a**) in quantitative yield. **3** is an air-stable solid; solutions, however, slowly react (over several days) with oxygen to give unidentified green solutions. **3a** is soluble in polar organic solvents and water. The crude product was recrystallized by slow evaporation of a 70/20/10 mixture of CH_2Cl_2/toluene/hexane and washed with 3–5 mL of cold CH_2Cl_2 to give red crystals in a yield of 60%.

Crystals of the BF_4^- salt (**3b**) were obtained by adding 0.052 g (0.27 mmol) of $AgBF_4$ (Aldrich) in 5 mL of MeOH to 0.100 g (0.125 mmol) of **3a** in 5 mL of MeOH. A yellow-orange precipitate immediately formed, which was filtered and washed with CH_2Cl_2 to give a clear yellow-orange solution, which was vacuum evaporated to dryness to give an orange-yellow solid. This was dissolved in MeOH and slowly evaporated to yield X-ray quality crystals of **3b**. Crystals of the PF_6^- salt can be obtained by the same procedure using $AgPF_6$.

Satisfactory elemental analyses (Galbraith Laboratories) could not be obtained for **3a** due to the CH_2Cl_2 solvents of crystallization. The BF_4^- salt (**3b**) also did not give satisfactory analyses despite attempts with crystalline samples. ^{31}P NMR for **3a** (CH_2Cl_2 with H_3PO_4 reference): δ 103.8 (pseudo-quintet, 2 P, J_{P-P} = 30 Hz), 56.2 (pseudo-doublet, 4 P, J_{P-P} = 44 Hz).

X-ray Crystallography for 3a. A well-formed red crystal of **3a** was mounted at the end of a glass fiber with epoxy. A total of 6313 independent reflections were collected at 22 °C on a Nicolet P3 diffractometer using Mo Kα radiation and the $\theta/2\theta$ scan data collection technique with a maximum 2θ angle of 45°. Three standard reflections measured every 100 data points showed no significant change in intensity. Data were corrected for Lorentz and polarization effects, but were not corrected for absorption or extinction. The structure was solved by using the Enraf-Nonius Structure Determination Package via the MULTAN direct-methods programs. The structure was refined by using 5441 reflections with $F_o^2 > 3\sigma(F_o^2)$ to give discrepancy indices of $R = 0.058$ and $R_w = 0.107$ for 388 variables representing 43 anisotropic non-hydrogen atoms. Table I lists information about the data collection and solution, while Tables II and IV list the positional parameters and selected bond distances and angles. Tables of anisotropic thermal parameters and a complete set of bond distances and angles are provided as supplementary material.

van der Waals Energy Calculations. The van der Waals calculations were done on a model system of **3a** derived from the crystallographic coordinates with methyl groups replacing the ethyl groups on the terminal phosphorus atoms. The only geometric parameters varied were rotations (5° increments) about the two P–CH_2–P bonds. No electrostatic factors were included in the energy calculations and both SYBYL and CHEMGRAF program packages gave essentially identical results.

X-ray Crystallography for 3b. A well-formed orange crystal of **3b** was mounted at the end of a glass fiber with epoxy. Mo Kα radiation and the ω-scan data collection technique were used to collect data with a maximum 2θ angle of 45°. Three standard reflections measured every

(1) Current address: Department of Chemistry, Louisiana State University, Baton Rouge, LA 70803-1804.
(2) Askham, F. R.; Stanley, G. G.; Marques, E. C. *J. Am. Chem. Soc.* **1985**, *107*, 7423.

0020-1669/87/1326-1177$01.50/0

Table I. Crystallographic Data for $Ni_2Cl_2(eHTP)^{2+}(Cl^-)_2 \cdot 2CH_2Cl_2$ (**3a**) and $Ni_2Cl_2(eHTP)^{2+}(BF_4^-)_2$ (**3b**)

	3a	**3b**
	Crystal Parameters	
formula	$Ni_2Cl_8P_6C_{27}H_{62}$	$Ni_2Cl_2P_6F_8C_{25}B_2H_{58}$
fw	971.67	906.52
cryst syst	monoclinic	monoclinic
space group	$P2_1/c$	$P2_1/c$
a, Å	18.347 (6)	11.679 (5)
b, Å	14.148 (5)	25.47 (1)
c, Å	17.660 (7)	14.069 (4)
β, deg	105.21 (1)	100.55 (3)
V, Å^3	4423 (4)	4113 (4)
Z	4	4
d_{calcd}, g/mL	1.46	1.39
μ(Mo Kα), cm^{-1}	15.77	13.34
temp, °C	22	25
cryst size, mm	0.75 × 0.50 × 0.35	0.50 × 0.30 × 0.2
cryst color	red	orange
	Data Collection and Structure Refinement	
diffractometer	Nicolet P3	Nicolet P3
radiation	Mo Kα	Mo Kα
monochromator	graphite crystal	graphite cryst
scan method	$\theta/2\theta$	ω
scan speed, deg/min	variable, 4–29	variable, 2–29
data limits, deg	$3 < 2\theta < 45$	$3 < 2\theta < 45$
octants collcd	$h,k,\pm l$	$h,k,\pm l$
Friedel pairs collcd	no	no
no. of reflcns collcd	6313	5786
no. of unique data $F_o^2 > 3\sigma(F_o^2)$	5441	3904
no. of params refined	388	424
data/param ratio	14.0	9.2
R^a	0.058	0.057
R_w^b	0.107	0.071
quality of fit indicator^c	3.00	1.83
largest final Fourier peak, e/Å^3	1.21	0.76
largest final shift/esd	0.6	0.5
abs cor	no	no

$^a R = \sum||F_o| - |F_c||/\sum|F_o|$. $^b R_w = [\sum_w(|F_o| - |F_c|)^2/\sum w|F_o|^2]^{1/2}$; $w = 1/\sigma(|F_o|)$. ^{c}Quality of fit $= [\sum w(|F_o| - |F_c|)^2/(N_{observn} - N_{params})]^{1/2}$.

100 data points showed no significant change in intensity. Data were corrected for Lorentz and polarization effects, but were not corrected for absorption or extinction. The structure was solved by using the MULTAN direct methods programs. The structure was refined by using 3904 reflections with $F_o^2 > 3\sigma(F_o^2)$ to give discrepancy indices of $R = 0.057$ and $R_w = 0.071$ for 424 variables representing 45 anisotropic and two isotropic non-hydrogen atoms. Two of the ethyl groups on eHTP were disordered; one was sucessfully modeled with isotropic thermal parameters while the other resulted in unusually large thermal parameters on the methyl carbon and a short C–C bond distance. Table I lists information about the data collection and solution, while Tables III and IV list the positional parameters and selected bond distances and angles. Tables of anisotropic thermal parameters and a complete set of bond distances and angles are provided as supplementary material.

Results and Discussion

The reaction of 2 equiv of $NiCl_2 \cdot 6H_2O$ with eHTP quantitatively yields the diamagnetic binuclear complex $Ni_2Cl_2(eHTP)^{2+}$ (**3**), which has been isolated in crystalline form as the chloride (**3a**) and BF_4^- (**3b**) salts. The ^{31}P NMR spectrum of **3** is very similar to that seen for the open-mode cobalt complex $Co_2(CO)_4(eHTP)^{2+}$ (**2**), which has a symmetrical eHTP conformation. An X-ray structure (Figure 1) on $Ni_2Cl_2(eHTP)^{2+}(Cl^-)_2$ (**3a**) reveals a distorted square-planar geometry about both nickel atoms with the eHTP ligand coordinating in a symmetrical bischelating, tridentate fashion. Selected bond distances and angles for **3a** are listed in Table IV. The local geometry about the nickel atoms is similar to that seen for the mononuclear complex, $[NiCl\{PhP(CH_2CH_2PPh_2)_2\}]^+$, except that the distortion away from square planar is more pronounced, with considerable differences even between each half of **3a**.[3] The *trans*-P–Ni–P angle is the most distorted with a value of 158.49 (4)° for P2–Ni1–P3, while P5–Ni2–P6 has a significantly larger angle of 166.50 (5)°.

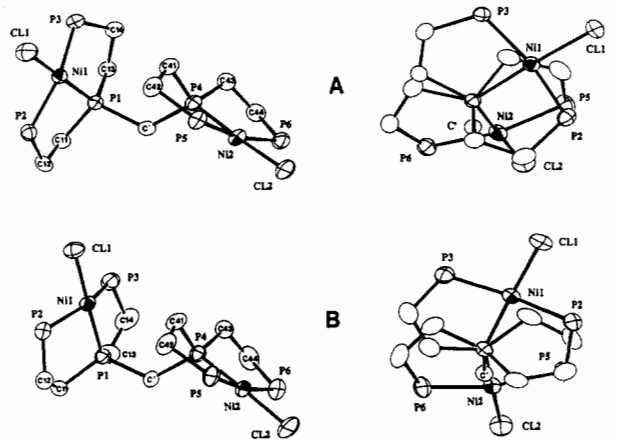

Figure 1. ORTEP plots of the $Ni_2Cl_2(eHTP)^{2+}$ portion of the chloride (**3a**) (A) and BF_4^- (**3b**) (B) complexes. The ethyl groups on the terminal phosphorus atoms have been omitted for clarity. Perpendicular views of the complexes are shown to clearly illustrate the rotational differences between the two species. Probability ellipsoids are shown at the 33% level.

The overall ligand configuration is about midway between the open-mode structures **1b** (syn–syn, W-shaped) and **1c** (syn–anti, scyth-shaped).[4]

The variation in the eHTP conformations between the cobalt and nickel complexes was intriguing, and we decided to examine

(3) Bertinsson, G.-I. *Acta Crystallogr., Sect. C: Cryst. Struct. Commun.* **1983**, *C39*, 563.

(4) Although the use of syn and anti notations is not technically accurate in the case of a saturated $M_2(eHTP)$ system, we will, nonetheless, use the terms to refer to the orientation of the metal atoms with respect to the protons on the central methylene bridge. Syn–syn will, therefore, designate that both metals are on the same side of the ligand as the methylene hydrogens.

Table II. Positional Parameters and Their Estimated Standard Deviations for $Ni_2Cl_2(eHTP)^{2+}(Cl^-)_2 \cdot 2CH_2Cl_2$ (**3a**)

atom	x	y	z	B,[a] Å²
Ni1	0.76834 (4)	0.48910 (5)	0.58878 (4)	2.91 (1)
Ni2	0.76204 (4)	0.89238 (5)	0.54693 (5)	3.39 (2)
Cl1	0.88077 (9)	0.4276 (1)	0.6318 (1)	4.94 (4)
Cl2	0.8079 (1)	1.0219 (1)	0.5096 (1)	4.80 (4)
Cl3	0.7334 (1)	0.7480 (2)	0.3493 (1)	6.59 (5)
Cl4	0.5288 (1)	0.2988 (1)	0.5381 (1)	5.10 (4)
P1	0.66375 (8)	0.5594 (1)	0.54331 (8)	2.81 (3)
P2	0.73423 (9)	0.4757 (1)	0.69996 (9)	3.34 (3)
P3	0.76633 (9)	0.4656 (1)	0.46439 (9)	3.84 (3)
P4	0.71989 (8)	0.7702 (1)	0.59181 (9)	3.19 (3)
P5	0.87251 (9)	0.8220 (1)	0.5740 (1)	3.93 (3)
P6	0.65647 (9)	0.9617 (1)	0.5499 (1)	3.92 (3)
C′	0.6728 (3)	0.6849 (4)	0.5175 (3)	3.3 (1)
C11	0.6016 (3)	0.5473 (4)	0.6083 (3)	3.3 (1)
C12	0.6491 (3)	0.5456 (5)	0.6938 (3)	3.7 (1)
C13	0.6157 (4)	0.5071 (5)	0.4487 (3)	3.9 (1)
C14	0.6734 (4)	0.4974 (5)	0.4010 (3)	4.1 (1)
C21	0.7072 (4)	0.3521 (4)	0.7049 (4)	4.5 (1)
C22	0.6843 (5)	0.3264 (6)	0.7791 (5)	6.8 (2)
C23	0.7944 (4)	0.5071 (5)	0.7969 (4)	4.7 (2)
C24	0.8648 (5)	0.4545 (7)	0.8256 (5)	6.5 (2)
C31	0.7783 (5)	0.3401 (5)	0.4500 (4)	5.6 (2)
C32	0.7237 (6)	0.2772 (6)	0.4786 (5)	7.0 (2)
C33	0.8322 (5)	0.5256 (6)	0.4167 (5)	6.7 (2)
C34	0.9102 (7)	0.5072 (9)	0.4445 (8)	10.0 (4)
C41	0.8009 (4)	0.7115 (4)	0.6591 (4)	4.0 (1)
C42	0.8639 (3)	0.7068 (5)	0.6180 (4)	4.4 (1)
C43	0.6483 (3)	0.8060 (5)	0.6406 (3)	3.9 (1)
C44	0.5975 (4)	0.8800 (4)	0.5872 (4)	4.2 (1)
C51	0.9150 (5)	0.8013 (6)	0.4942 (5)	6.0 (2)
C52	0.9908 (5)	0.7507 (7)	0.5174 (6)	8.1 (2)
C53	0.9423 (4)	0.8871 (5)	0.6487 (5)	5.6 (2)
C54	0.9217 (5)	0.9084 (6)	0.7222 (5)	7.0 (2)
C61	0.6690 (6)	1.0665 (6)	0.6126 (6)	8.1 (2)
C62	0.6948 (9)	1.0496 (9)	0.6920 (7)	11.4 (4)
C63	0.5999 (4)	1.0070 (5)	0.4586 (5)	6.0 (2)
C64	0.5824 (6)	0.9344 (8)	0.3960 (6)	7.5 (2)
C1	0.4681 (5)	0.2734 (7)	0.7101 (5)	6.3 (2)
Cl5	0.4798 (1)	0.3912 (2)	0.7404 (1)	7.01 (6)
Cl6	0.5125 (1)	0.1961 (2)	0.7898 (2)	9.31 (7)
C2	0.9103 (7)	0.3177 (7)	0.1722 (6)	9.6 (3)
Cl7	0.8906 (2)	0.3220 (2)	0.2641 (2)	10.5 (1)
Cl8	1.0029 (2)	0.3464 (3)	0.1788 (2)	10.35 (9)

[a] *B* values for anisotropically refined atoms are given in the form of the isotropic equivalent displacement parameter defined as $^4/_3$ [$a^2B(1,1) + b^2B(2,2) + c^2B(3,3) + ab(\cos\gamma)B(1,2) + ac(\cos\beta)B(1,3) + bc(\cos\alpha)B(2,3)$].

Table III. Positional Parameters and Their Estimated Standard Deviations for $Ni_2Cl_2(eHTP)^{2+}(BF_4^-)_2$ (**3b**)

atom	x	y	z	B,[a] Å²
Ni1	0.60805 (7)	0.06655 (3)	0.70403 (6)	3.34 (2)
Ni2	0.83468 (7)	0.23015 (3)	0.97501 (6)	3.52 (2)
Cl1	0.5464 (2)	0.08217 (8)	0.5514 (1)	5.15 (4)
Cl2	0.8725 (2)	0.29197 (8)	1.0836 (2)	6.16 (5)
P1	0.6680 (1)	0.05543 (6)	0.8545 (1)	3.22 (3)
P2	0.4334 (2)	0.07661 (7)	0.7390 (1)	4.08 (4)
P3	0.7640 (2)	0.02365 (8)	0.6803 (1)	4.55 (4)
P4	0.7957 (2)	0.16834 (6)	0.8739 (1)	3.45 (3)
P5	0.6687 (2)	0.26562 (7)	0.9053 (2)	4.36 (4)
P6	1.0088 (2)	0.19520 (8)	1.0128 (2)	4.83 (5)
F1	0.0776 (4)	0.5464 (2)	0.4140 (3)	7.6 (1)
F2	0.2593 (4)	0.5355 (2)	0.3867 (4)	8.0 (1)
F3	0.1078 (4)	0.5432 (2)	0.2611 (3)	7.8 (1)
F4	0.1277 (5)	0.4713 (2)	0.3506 (4)	8.4 (2)
F5	0.4299 (6)	0.3072 (3)	0.6486 (5)	11.9 (2)
F6	0.3485 (6)	0.3405 (3)	0.5128 (5)	14.2 (2)
F7	0.5359 (6)	0.3497 (3)	0.5590 (5)	12.8 (2)
F8	0.4168 (9)	0.3945 (3)	0.6266 (8)	17.3 (3)
C′	0.7288 (5)	0.1133 (2)	0.9266 (5)	3.4 (1)
C11	0.5458 (6)	0.0373 (3)	0.9125 (5)	4.5 (2)
C12	0.4397 (6)	0.0699 (3)	0.8693 (5)	5.3 (2)
C13	0.7754 (7)	0.0032 (3)	0.8721 (5)	5.4 (2)
C14	0.8466 (7)	0.0043 (3)	0.7962 (6)	6.3 (2)
C21	0.3424 (7)	0.0238 (3)	0.6804 (5)	5.3 (2)
C22	0.3949 (8)	−0.0302 (3)	0.6962 (6)	6.6 (2)
C23	0.3483 (7)	0.1361 (3)	0.6985 (7)	6.5 (2)
C24	0.237 (1)	0.1416 (5)	0.734 (1)	11.8 (4)
C31	0.888 (1)	0.0476 (7)	0.633 (1)	6.3 (4)
C31′	0.845 (2)	0.0613 (8)	0.591 (1)	7.7 (5)
C32′	0.963 (2)	0.050 (1)	0.601 (2)	11.0 (7)
C32	0.857 (2)	0.0599 (7)	0.520 (1)	6.4 (4)
C33	0.7144 (8)	−0.0366 (3)	0.6178 (6)	6.3 (2)
C34	0.804 (1)	−0.0727 (4)	0.5900 (7)	8.7 (3)
C41	0.6912 (7)	0.1907 (3)	0.7688 (5)	4.9 (2)
C42	0.5983 (7)	0.2221 (3)	0.8071 (6)	5.2 (2)
C43	0.9299 (6)	0.1455 (3)	0.8399 (5)	4.9 (2)
C44	1.0189 (6)	0.1387 (3)	0.9337 (7)	5.8 (2)
C51	0.6884 (8)	0.3287 (3)	0.8499 (7)	6.3 (2)
C52	0.m69 (1)	0.3280 (4)	0.7776 (9)	10.4 (3)
C53	0.5625 (7)	0.2777 (4)	0.9820 (7)	6.9 (2)
C54	0.4397 (8)	0.2939 (5)	0.9290 (9)	10.2 (3)
C61	1.1215 (8)	0.2399 (3)	0.9941 (9)	9.0 (3)
C62	1.106 (1)	0.2672 (6)	0.911 (1)	16.3 (5)
C63	1.045 (1)	0.1704 (5)	1.1406 (8)	11.6 (3)
C64	1.146 (2)	0.1597 (9)	1.177 (1)	21.4 (8)
B1	0.1430 (7)	0.5237 (4)	0.3528 (6)	5.1 (2)
B2	0.432 (1)	0.3488 (5)	0.5907 (9)	7.5 (3)

[a] *B* values for anisotropically refined atoms are given in the form of the isotropic equivalent displacement parameter defined as $^4/_3$ [$a^2B(1,1) + b^2B(2,2) + c^2B(3,3) + ab(\cos\gamma)B(1,2) + ac(\cos\beta)B(1,3) + bc(\cos\alpha)B(2,3)$].

the van der Waals energy differences for rotations about the central methylene–phosphorus bonds in **3a** using the CHEMGRAF[5] and SYBYL[6] molecular graphics/mechanics programs. The results of these simple van der Waals energy calculations confirm that the crystal structure is indeed the lowest energy configuration, but there are three other possible rotomers within 4 kcal from that observed crystallographically.

The calculations are summarized in Figure 2, which shows a contour plot of an expanded portion of the 360° × 360° van der Waals energy map. The contours represent increments in the van der Waals energies of 5.0 kcal/mol up to a maximum of 20 kcal/mol, while the axes are rotation angles about the two central methylene–phosphorus bonds. The origin of the plot (0°, 0°), which is not shown in Figure 2, represents angular values corresponding to the closed-mode configuration **1a**. An interesting result of the calculation is that the closed-mode form is *not* sterically accessable for a *square-planar* eHTP coordination mode, which is what we had suspected from the use of molecular models. In order to allow formation of the closed-mode form, the terminal phosphine atoms must be *cisoidal*.

The calculation clearly shows that there are four low-energy regions with the crystallographically observed rotomer, **3a**, residing in the center of region A of the diagram. The next lowest energy rotomer falls in region B of the diagram and is an open-mode form similar to **1c**, which has a van der Waals energy of only +0.9 kcal/mol above that of **3a**. The two regions labeled C are symmetric conformers of **1b** with a relative van der Waals energy of +2.2 kcal/mol, while region D, which is not shown on Figure 2, represents an intermediate structure between the conformations of **3a** and **1b** with a van der Waals energy of +3.2 kcal/mol above that seen for **3a**.

Aside from identifying favored low-energy configurations for our binuclear, square-planar nickel eHTP complex, the calculations also give valuable information about the availability of energetically reasonable pathways from one rotomer to another. Since the torsional energies involved for rotations about single bonds are minimal, the van der Waals energies should be the primary contributing factors to any rotational barrier. The calculations

(5) (a) Davies, E. K. "CHEMGRAF Program Suite", Chemical Crystallography Laboratory, University of Oxford, England, 1982. (b) Newsam, J. M. ; Halbert, T. R. *Inorg. Chem.* **1985**, 24, 491.

(6) (a) Naruto, S.; Motoc, I.; Marshall, G. R.; Daniels, S. B.; Sofia, M. J.; Katzenellenbogen, J. A. *J. Am. Chem. Soc.* **1985**, *107*, 5262. (b) The SYBYL program package is available from TRIPOS Associates, St. Louis, MO 63117.

Table IV. Selected Bond Distances (Å) and Angles (deg) for $Ni_2Cl_2(eHTP)^{2+}$ (**3a** = Cl^- Salt, **3b** = BF_4^- Salt)[a,b]

	3a	3b
Ni1–Ni2	5.7505 (6)	5.9333 (8)
Ni1–Cl1	2.183 (1)	2.173 (1)
Ni1–P1	2.1232 (9)	2.123 (1)
Ni1–P2	2.220 (1)	2.199 (2)
Ni1–P3	2.212 (1)	2.202 (2)
Ni2–Cl2	2.189 (1)	2.182 (2)
Ni2–P4	2.130 (1)	2.114 (1)
Ni2–P5	2.195 (1)	2.200 (2)
Ni2–P6	2.184 (1)	2.194 (2)
P1–C′	1.851 (3)	1.855 (5)
P4–C′	1.825 (4)	1.827 (5)
Cl1–Ni1–P1	174.84 (4)	177.11 (6)
Cl1–Ni1–P2	96.79 (4)	92.68 (6)
Cl1–Ni1–P3	93.08 (4)	94.26 (6)
P1–Ni1–P2	86.44 (4)	86.71 (6)
P1–Ni1–P3	85.23 (4)	87.38 (6)
P2–Ni1–P3	158.49 (4)	156.77 (6)
Cl2–Ni2–P4	175.83 (5)	177.72 (7)
Cl2–Ni2–P5	92.22 (4)	93.73 (6)
Cl2–Ni2–P6	92.59 (4)	93.62 (6)
P4–Ni2–P5	87.46 (4)	86.69 (5)
P4–Ni2–P6	86.82 (4)	86.37 (6)
P5–Ni2–P6	166.50 (5)	167.56 (7)
P1–C′–P4	120.9 (2)	122.5 (3)

[a] Numbers in parentheses are estimated standard deviations in the least significant digits. [b] A complete set of bond distances and angles is given in the supplementary material.

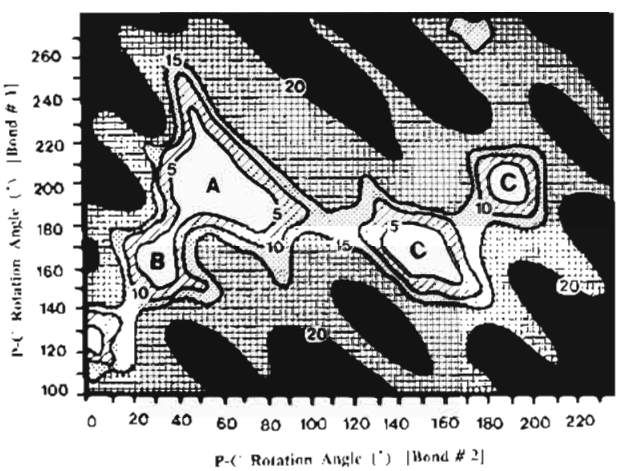

Figure 2. An expanded portion of the full 360° × 360° van der Waals energy rotational map from the SYBYL program set for a model complex of **3a** with methyl groups on the terminal phosphorus atoms instead of ethyl groups. Axes indicate rotational angles about the two P–CH_2–P bonds with contours showing relative van der Waals energy values. Each contour represents 5.0 kcal and the four local minima, in terms of increasing energies, are labeled A, B, C, and D. Region A indicates the location of the structurally determined rotomer for the chloride salt (**3a**) while region B corresponds to the rotomer for the BF^{4-} salt (**3b**). See text for further details.

indicate that there are relatively low barriers for rotations from regions D → B → A → C. The lowest energy pathway is from region A to region B with a barrier of only 4.3 kcal/mol.

The small energy difference and rotational barrier between **3a** and the other rotomers points to the probable existence of facile rotations about the central methylene group.[7] Since we had

(7) We feel that, in general, the results from the van der Waals energy calculations represent a rough upper limit since the calculation assumes a static, inflexible molecule (except for the rotated bonds). Other crystal structures and solution NMR data on eHTP complexes clearly indicate that these open-mode systems enjoy considerable flexibility in the P–CH_2–P bond angle and metal phosphorus chelate rings. The likely effect of this flexibility would be to lower pathway barriers between rotomers from that calculated from our simple model.

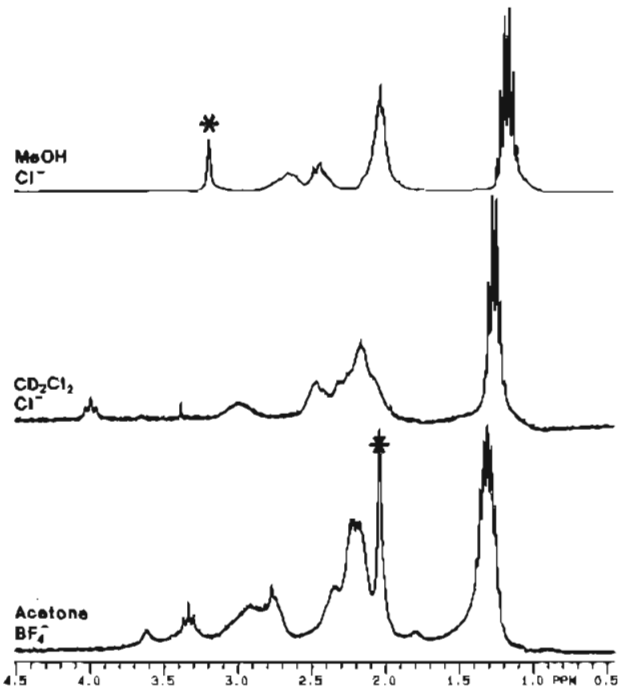

Figure 3. 300-MHz ^1H NMR spectra of **3** at 28 °C. Solvents (all deuteriated) and counteranions are indicated for each spectrum. Peaks marked with an asterisk are due to solvent. The multiplet located between 1.1 and 1.4 ppm is due to the CH_3 protons of the eHTP ethyl groups, the multiplet between 2.0 and 2.4 is primarily due to the CH_2 protons of the ethyl groups, the signals between 2.4 and 3.0 ppm are due to the bridging ethylene group protons, and the downfield triplet pattern in the CD_2Cl_2 and acetone solvent systems is due to the central bridging CH_2 protons. In MeOH this signal is probably in the 2.4–2.8 ppm region, although we have not yet fully assigned it by 2-dimensional and phosphorus-decoupled NMR techniques.

obtained X-ray quality single crystals of the BF_4^- salt (**3b**), another crystal structure was performed to see if crystal packing forces would induce a rotation about the central P–CH_2–P linkage and whether this would correspond to any of the low-energy conformers predicted from the van der Waals energy calculations. An ORTEP plot of the BF^{4-} salt (**3b**) is shown in Figure 1 with selected bond distances and angles listed in Table IV. The major difference between the two structures is that the eHTP ligand does indeed adopt a substantially different rotomeric conformation about the central P–CH_2–P linkage. Moreover, this rotational form agrees well with that predicted from the van der Waals calculations as the second lowest energy configuration, namely, the syn–anti form **1c** (region B in Figure 2).

One of the clearest indicators of the differences between the two rotomeric forms is the Ni1–P1–P4–Ni2 torsional (dihedral) angle: 93° for **3a** and 146° for **3b**. The M–M contact distance is also related to the rotational form with **3a** having a Ni–Ni distance of 5.7505 (6) Å, while **3b** has a distance of 5.9333 (8) Å. These are both considerably less than that seen for the syn–syn conformation **1b** in which the metal centers are at their greatest possible separation (6.697 (1) Å in the cobalt complex **2**). Another interesting difference between the nickel and cobalt structures are the smaller P–CH_2–P angles of 120.9 (2) (**3a**) and 122.5 (3)° (**3b**) vs. the rather large value of 127.7 (3)° for **2**.

The ^1H NMR of **3** definitely indicates that the molecule is exhibiting some sort of dynamic behavior in solution. The ^1H NMR peaks for **3** show, for example, a marked solvent and, in some cases, anion dependence as illustrated in Figure 3. These differences, we believe, result from two different processes that can occur for **3**: in the presence of chloride anions one can have chloride association and dissociation occurring, which gives rise to an equilibrium between the neutral 5-coordinate $Ni_2Cl_4(eHTP)$ complex and **3**; the second process involves rotational motion about the central methylene bridge of the eHTP ligand allowing interconversion of the various rotomers of **3**. Solvent effects could

easily differentiate (or set up dynamic equilibria between) the various conformers seen from the van der Waals energy calculations. Some of these conformers are expected to have different enough local chemical environments for the central methylene and bridging ethylene protons to give rise to the ^{1}H NMR spectra seen in Figure 3.[8]

The qualitative, almost quantitative, agreement of the simple van der Waals energy calculations with the solid-state structures and solution dynamics is rather impressive and opens the door for more detailed NMR studies into these and other eHTP complexes. We are currently examining the reactions of **3** relative to those of mononuclear model complexes to see if this type of binuclear system can exhibit cooperative behavior between the metal centers for C–C bond-forming reactions in alkenes.

Acknowledgment. We thank the donors of the Petroleum Research Fund, administered by the American Chemical Society, and the National Science Foundation (Grant CHE-86-13089) for research support. We also acknowledge Monsanto Co. for a Young Faculty Research Support Grant. The assistance of the Washington University High-Resolution NMR Service Facility, funded in part through NIH Biomedical Research Support Shared Instrument Grant 1-S10-RR02004 and a gift from the Monsanto Co., is gratefully acknowledged.

Registry No. **3** (PF_6^- salt), 106973-26-6; **3a**, 106905-68-4; **3b**, 106973-25-5.

Supplementary Material Available: Figure of the full van der Waals energy map and tables of anisotropic thermal parameters, complete bond distances, and complete bond angles for both **3a** and **3b** (9 pages); tables of observed vs. calculated structure factors for both **3a** and **3b** (35 pages). Ordering information is given on any current masthead page.

(8) The cobalt complex (**2**) also exhibits marked solvent dependencies (although no anion effects have been observed) for its ^{1}H NMR spectra. We are currently concluding detailed two-dimensional studies on the cobalt system and plan to explore the nickel system in more detail: D'Avignon, A.; Askham, F. R.; Stanley, G. G., manuscript in preparation (cobalt system).

Contribution from the Department of Chemistry,
University of British Columbia,
Vancouver, British Columbia, Canada V6T 1Y6

Synthesis and Reactivity of Five-Coordinate (Porphinato)(tertiary phosphine)ruthenium(II) Complexes

Chand Sishta, Mark J. Camenzind, Brian R. James,* and David Dolphin*

Received December 5, 1986

Coordinatively unsaturated ruthenium porphyrin complexes such as $[Ru(porp)]_2$ (porp = dianion of 2,3,7,8,12,13,17,18-octaethylporphyrin (OEP) or 5,10,15,20-tetraphenylporphyrin (TPP)),[1] $K_2[Ru(porp)]$ (porp = OEP or 5,10,15,20-tetratolylporphyrin dianion),[2] Ru(TMP) (TMP = dianion of 5,10,15,20-tetramesitylporphyrin),[3] Ru(OEP)R (R = $CHCH_3$ and C_2H_5,[4] CH_3 and C_6H_5[5]) and the in situ hydride[6] $[RuH(TTP)]^-$ have been reported recently. This note describes the synthesis, characterization, and some chemistry of the analytically pure complexes $Ru(porp)(PR_3)$ (**2**, porp = TMP, R = *n*-Bu; **4**, porp = OEP, R = Ph); such 16-electron species, formed in situ by dissociation

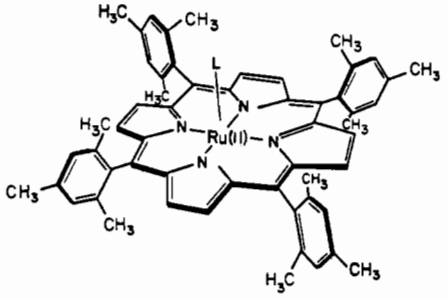

2, L = *n*-Bu_3P

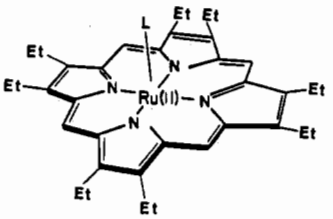

4, L = PPh_3

equilibria involving $Ru(porp)(PR_3)_2$,[7,8] have been implicated as intermediates in catalytic oxidation of phosphines[8] and decarbonylation of aldehydes.[9] Reaction of **2** or **4** with CO or PR_3 gives the expected six-coordinate derivatives, while aerobic treatment with HBr gives $RuBr(porp)(PR_3)$; **2** and **4** are unreactive toward O_2, N_2, H_2, and aldehydes, and the implications of this nonreactivity for the reported catalysis are discussed.

Experimental Section

^{1}H and ^{31}P NMR spectra were obtained in C_6D_6 in vacuo, with Varian XL-300 and Bruker WP-80 and WH-400 spectrometers, and shifts are reported relative to Me_4Si or 85% H_3PO_4, downfield shifts being positive. Visible spectra were run on a Cary 17D spectrophotometer.

Ru(TMP)(*n*-Bu_3P)$_2$ (1). The carbonyl Ru(TMP)(CO) (170 mg, 0.19 mmol), prepared by a literature method,[10] was dissolved in 20 mL of CH_2Cl_2 under N_2, and *n*-Bu_3P (0.34 mL, 1.4 mmol) was added. The solution was refluxed under N_2 until the visible spectrum of the carbonyl (λ_{max} 412, 524 nm) changed to that of **1**. After reduction of the solution volume to 5 mL by evaporation, dropwise addition of MeOH (15 mL) precipitated a purple powder that was filtered off, washed with MeOH, and dried under vacuum (200 mg, 84%). Anal. Calcd for $C_{80}H_{106}N_4P_2Ru$: C, 74.67; H, 8.30; N, 4.35. Found: C, 74.63; H, 8.22; N, 4.37. ^{1}H NMR: δ 8.43 s (8 H, pyrrole H), 7.23 s (8 H, *m*-H), 2.48 s (12 H, *p*-CH_3), 2.43 s (24 H, *o*-CH_3), 0.54 m (12 H, CH_2CH_3), 0.46 t (18 H, CH_2CH_3), −0.44 br (12 H, PCH_2CH_2), −1.79 br, t (12 H, PCH_2). ^{31}P NMR: δ −0.38 s. UV/visible (CH_2Cl_2): λ_{max} 437, 530, 562 nm.

Ru(TMP)(*n*-Bu_3P) (2). Complex **1** (60 mg, 0.05 mmol), on pyrolysis for 1 h at 270 °C under a 4×10^{-5} Torr vacuum loses phosphine and forms **2** quantitatively. Anal. Calcd for $C_{68}H_{79}N_4PRu$: C, 75.31; H, 7.34; N, 5.17. Found: C, 75.05; H, 7.33; N, 5.20. ^{1}H NMR: δ 8.45 s (8 H, pyrrole H), 7.29 s (4 H, *m*-H), 7.12 s (4 H, *m*-H), 2.63 s (12 H, *p*-CH_3), 2.47 s (12 H, *o*-CH_3), 1.72 s (12 H, *o*-CH_3), 0.43 m (15 H, CH_2CH_3), −0.64 m (6 H, PCH_2CH_2), −1.54 m (6 H, PCH_2). ^{31}P NMR: δ 53.09 s. UV/visible (CH_2Cl_2): λ_{max} 410, 498, 523 nm.

Ru(OEP)(PPh_3)$_2$ (3). Complex **3** was prepared according to the literature procedure.[7] ^{1}H NMR: δ 9.12 s (4 H, meso H), 6.57 t (6 H, *p*-H), 6.36 m (12 H, *m*-H), 4.36 m (12 H, *o*-H), 3.75 q (16 H, CH_2), 1.89 t (24 H, CH_3). ^{31}P NMR: δ 8.31 s.

(1) Collman, J. P.; Barnes, C. E.; Swepston, P. N.; Ibers, J. A. *J. Am. Chem. Soc.* **1984**, *106*, 3500.
(2) Collman, J. P.; Brothers, P. J.; McElwee-White, L.; Rose, E.; Wright, L. J. *J. Am. Chem. Soc.* **1985**, *107*, 4570.
(3) Camenzind, M. J.; James, B. R.; Dolphin, D. *J. Chem. Soc., Chem. Commun.* **1986**, 1137.
(4) Collman, J. P.; McElwee-White, L.; Brothers, P. J.; Rose, E. *J. Am. Chem. Soc.* **1986**, *108*, 1332.
(5) James, B. R. Presented at the 24th International Conference on Coordination Chemistry, Athens, Greece, 1986; abstracts, p 28. Ke, M.; Rettig, S. J.; James, B. R.; Dolphin, D., to be submitted for publication.
(6) Collman, J. P.; Brothers, P. J.; McElwee-White, L.; Rose, E. *J. Am. Chem. Soc.* **1985**, *107*, 6110.
(7) Ariel, S.; Dolphin, D.; Domazetis, G.; James, B. R.; Leung, T. W.; Rettig, S. J.; Trotter, J.; Williams, G. M. *Can. J. Chem.* **1984**, *62*, 755.
(8) James, B. R.; Mikkelsen, S. R.; Leung, T. W.; Williams, G. M.; Wong, R. *Inorg. Chim. Acta* **1984**, *85*, 209.
(9) (a) Domazetis, G.; Tarpey, B.; Dolphin, D.; James, B. R. *J. Chem. Soc., Chem. Commun.* **1980**, 939. (b) Domazetis, G.; James, B. R.; Tarpey, B.; Dolphin, D. *ACS Symp. Ser.* **1981**, *No. 152*, 243.
(10) Groves, J. T.; Quinn, R. *Inorg. Chem.* **1984**, *23*, 3844.

0020-1669/87/1326-1181$01.50/0